

## Lumped Vortex Element Flying Over Free Water Surface

Sakir Bal <sup>1</sup> Istanbul Technical University Department of Naval Architecture and Marine Engineering, Maslak, Istanbul, Türkiye.

**Abstract:** In this study, the lift coefficients (circulation) of two-dimensional flat-plate flying with a constant speed over a free surface have been calculated by a closed-form (analytical) solution. The effects of very high speed have also been included in the calculations. The flat-plate has been modeled by a lumped vortex element under the conditions of potential flow theory. While the kinematic boundary condition (zero normal velocity condition) is satisfied at three-quarter chord length of flat-plate, linearized and combined (kinematic and dynamic) condition has been applied on the free water surface. The total velocity potential has then been calculated by the method of images. Kutta condition is satisfied automatically at the trailing edge by this lumped vortex element. The wave elevations on the free surface have also been calculated in a closed-form solution. First, the lift coefficient by the present analytical solution have been validated with those of another numerical method for NACA0004 foil section. Later, the effects of Froude number, clearance (vertical distance) of flat-plate from calm free water surface, and the angle of attack on the results (namely lift coefficients and free surface deformations) have been discussed in a detailed manner. It has been found that the lift coefficient varies significantly with Froude number particularly for lower clearance values. An increase in Froude number causes also an increase both in wave-length and in wave-height on the free surface. On the other hand, a decrease in clearance (means a closer distance to free surface) causes an increase in wave-height but not in wave-length. A similar finding is noted for angle of attack. An increase in angle of attack causes an increase in loading as well as in wave-height but not in wave-length.

**Keywords:** Lumped vortex element, free surface, wave deformation, lift coefficient, Froude number.

### Serbest Su Yüzeyinin Üzerinde Uçan Yoğunlaştırılmış Girdap Elemanı

**Özet:** Bu çalışmada, serbest su yüzeyi üzerinde sabit bir hızla uçan (hareket eden) iki boyutlu düz bir levhanın kaldırma kuvveti (sirkülasyon değeri) katsayısı kapalı (analitik) bir çözümle hesaplanmıştır. Çok yüksek hızlar da hesaplamalara dâhil edilmiştir. Düz levha, potansiyel akım teorisi göz önüne alınarak yoğunlaştırılmış girdap elemanı ile modellenmiştir. Kinematik sınır şartı (sıfır normal hız şartı) düz levhanın üç çeyrek giriş boyu mesafesinde sağlanırken, lineer ve kinematik-dinamik birleştirilmiş bir koşul serbest su yüzeyinde uygulanmıştır. Daha sonra, probleme ait toplam hız potansiyeli ayna simetriği yöntemiyle elde edilebilmiştir. Bu yoğunlaştırılmış girdap elemanı modelinde, Kutta şartı otomatik olarak sağlanmaktadır. Yine, serbest su yüzeyindeki dalga deformasyonları da kapalı bir çözüm olarak hesaplanmıştır. İlk olarak, NACA0004 foil geometrisi kullanılarak mevcut analitik çözümle hesaplanan kaldırma kuvveti katsayısı, diğer sayısal bir yöntemle bulunan kaldırma kuvveti katsayısı ile karşılaştırılmış ve gerekli doğrulama çalışması yapılmıştır. Daha sonra, Froude sayısının, düz levha ile serbest su yüzeyi arasındaki düşey mesafenin ve hücum açılarının sonuçlar (kaldırma kuvveti ve su yüzeyi deformasyonları) üzerindeki etkileri ayrıntılı bir biçimde tartışılmıştır. Özellikle, düşük düz levha-serbest su yüzeyi arası mesafede, Froude sayısının kaldırma kuvveti katsayısı üzerinde çok önemli değişikliklere neden olduğu bulunmuştur. Ayrıca artan Froude sayısı ile, serbest su yüzeyinde hem dalga boyunun hem de dalga yüksekliğinin arttığı görülmüştür. Düz levha serbest su yüzeyine yaklaştıkça, dalga yüksekliğinin arttığı ancak dalga boyunun değişmediği gözlemlenmiştir. Benzer bir sonuç hücum açısı için de not edilmiştir. Hücum açısındaki artış düz levha üzerindeki yüklemeyi ve dalga yüksekliğini artırmaktadır, ancak dalga boyunda herhangi bir değişime neden olmamaktadır.

**Anahtar Kelimeler:** Yoğunlaştırılmış girdap elemanı, serbest yüzey, dalga deformasyonu, kaldırma kuvveti katsayısı, Froude sayısı.

#### RESEARCH PAPER

Corresponding Author: Sakir BAL, [sbal@itu.edu.tr](mailto:sbal@itu.edu.tr).

**Citation:** Bal, S., (2023), Lumped Vortex Element Flying Over Free Water Surface, ITU ARI Bulletin of the Istanbul Technical University 55(1) 1–6,

**Submission Date:** 24 March 2023

**Online Acceptance :** 22 April 2023

**Online Publishing :** 24 April 2023

### 1.Introduction

Air wings (lifting surfaces) can help the marine vehicles support the weight of craft fully or partially at high speeds. Marine vehicles with WIG (wing-in-ground) effect, some racing and sport boats, including catamarans with hydrofoils and other air-assisted marine crafts can take this advantage of air wings. In this study, a closed-form (analytical) solution has been developed for the performance analysis of 2-D (two-dimensional) flat plate flying (moving) with a constant speed above free water surface. To do this, a lumped-vortex element has been utilized. To the best of the author’s knowledge, there is no such study in the literature.

In the past, 2-D WIG that is moving over free surface has been investigated numerically in (Zong et al., 2012). It was reported in this study that the WIG effect is significant when the clearance (distance between WIG and free water surface) is small and the free surface behaves like a rigid wall at high velocity of WIG. The problem of 2-D biplanes (with WIG effect) working near a free water surface was solved by extending the classical lifting theory in (Liang et al. 2013a). In this study, 3-D (three-dimensional) problem was also solved. Some extensive numerical results were presented for the effect of clearance (height from free surface) and the distance between two foils on the results (such as, lift coefficient, drag coefficient, etc.). Both 2-D and 3-D WIG problems were also solved (Barber, 2007). It was demonstrated that for low Froude numbers ( $Fr < 1$ ), the surface deformation is a small depression of the surface beneath the foil. If the Froude number increases, a small change in the shape of the deformation is observed. At higher Froude numbers (for instance, say a Froude number of 14), the surface is not a depression anymore, but rather a rise beneath the foil. It was expressed that this result was also consistent with that of shown before (Grundy 1986). Matveev (2014) has described a coupled aero-hydrodynamic model for a ram wing moving above water under the condition of steady motion. The factors affecting the aerodynamic performance of a ram wing and the associated water surface deformations have been presented in the study. It has been shown that an extent of blockage of wing sides can drastically change the ram wing lifting performance. In another study, the effects of free surface both on 2-D airfoils and 3-D wings moving steadily over a free surface have been investigated by an iterative numerical method (Bal, 2016). It was concluded in the study that free surface can affect the airfoil or wing performance drastically if the clearance is sufficiently small. In addition, Bal (2018) showed that tapered 3-D wing with different swept angles and dihedral angles under WIG effect were investigated numerically. It was found that the shape of wing is important in terms of its performance under certain conditions. An in-depth review on the research and development of WIG effect technology can be found in Rozhdestvensky’s work (2006).

There are also more advanced methods such as nonlinear numerical methods and CFD (Computational Fluid Dynamics) to solve the problem (Dogrul and Bal, 2016), (Kinaci and Bal, 2016), (Liang et al., 2013b), (Zhi et al., 2019) (Hu et al., 2021). They generate quite realistic solutions. All these methods are robust and reliable. However, they require computational time and memory. On the other hand, lumped vortex element is a very simple and effective representation of flat-plate (Katz and Plotkin, 2001). The lumped vortex element automatically satisfies the Kutta condition at the trailing edge of flat-plate and gives the exact solution of the problem (Katz, 2019). In this study the flat-plate moving steadily over a free surface have been represented by a lumped vortex element and closed-form solutions have been developed both for lift coefficients and free surface deformations.

### 2. Mathematical Formulation

A boundary value problem can be defined to solve the steady uniform flow passing a two-dimensional flat-plate flying over a free water surface. The flow field is assumed to be incompressible, inviscid, and irrotational. Therefore, potential flow theory can be applied. The x-axis is positive in the direction

of uniform inflow (U) and the z-axis is positive upwards as shown in Figure 1. The flat-plate is located above calm free surface at  $z = h$ . The governing equation is the Laplace equation that the perturbation potential,  $\phi$  (in terms of the total potential,  $\Phi = Ux + \phi$ ) should satisfy the continuity equation in the fluid domain:

$$\nabla^2 \phi(x, z) = 0 \tag{1}$$

The following boundary conditions should also be satisfied by the perturbation potential function  $\phi$ :

Linearized free surface condition: The following combined (kinematic and dynamic) and linearized free surface equation should be satisfied by the perturbation potential function:

$$\frac{\partial^2 \phi}{\partial x^2} + k_0 \frac{\partial \phi}{\partial z} = 0 \quad \text{on } z = 0 \tag{2}$$

Here,  $k_0=g/U^2$  is the wave number, and g is the gravitational acceleration. The corresponding wave elevation in linearized form from Bernoulli equation can also be given as follows:

$$\zeta = -\frac{U}{g} \frac{\partial \phi}{\partial x} \tag{3}$$

Radiation condition: There should be no upstream waves. This means that the potential function should satisfy the following both equations:

$$\lim_{x \rightarrow -\infty} \phi \rightarrow 0 \quad \text{and} \quad \lim_{x \rightarrow \infty} \phi \rightarrow M \tag{4}$$

Here M is a finite number. Refer to (Bal and Kinnas, 2002) and (Bal et al., 2001) for details.

The Kutta condition and kinematic condition on flat-plate are explained below.

### 3. Method of Solution

The flat-plate has been modeled by a lumped vortex element as mentioned above (Katz and Plotkin, 2001). To do this, the sum of the distributed vortices on flat-plate is replaced by a simple single (point) vortex with strength  $\Gamma$ . It is placed at the quarter-chord point of the flat-plate and the kinematic boundary condition (i.e. the zero normal velocity condition) is satisfied at the three-quarter chord point (Katz and Plotkin, 2001). The Kutta condition at the trailing edge of flat-plate is therefore satisfied automatically. The method of images was then utilized to satisfy the linearized free surface condition. The potential function  $\phi_1$  for a single vortex with strength  $\Gamma$ , located at  $z = h$  can be written as:

$$\phi_1(x, z) = -\frac{\Gamma}{2\pi} \tan^{-1} \left( \frac{h-z}{x} \right) \tag{5}$$

By using the following integral equation (Gradshteyn and Ryzhik, 1965):

$$\int_0^{\infty} e^{-k(h-z)} \sin(kx) dk = \frac{x}{x^2 + (h-z)^2} \tag{6}$$

and taking the derivative of Equation (5) with respect to z,  $\phi_1$  can be re-written as:

$$\phi_1(x, z) = \frac{\Gamma}{2\pi} \int_0^{\infty} \frac{e^{-k(h-z)} \sin(kx)}{k} dk \tag{7}$$

It is assumed that the perturbation potential,  $\Phi(x,z)$  is equal to  $\phi_1 + \phi_2 + \phi_3$ . Here,  $\phi_2$  is the potential function due to the mirror image of single vortex with the same strength  $\Gamma$  but in the opposite direction of rotation. It is located  $z=-h$ . Moreover,  $\phi_3$  is the gravitational wave potential and can be calculated by using the free surface condition, Equation (2), as follows:

$$\phi_2(x, z) = \frac{\Gamma}{2\pi} \tan^{-1} \left( \frac{z+h}{x} \right) = -\frac{\Gamma}{2\pi} \int_0^\infty \frac{e^{-k(z+h)} \sin(kx)}{k} dk \quad (8)$$

$$\phi_3(x, z) = \frac{\Gamma}{\pi} \int_0^\infty \frac{e^{-k(h-z)} \sin(kx)}{k - k_0} dk \quad (9)$$

For the evaluation of definite integral I, in Equation (9), the method of solution given by Hess and Smith (1966) has been adopted here. The integral, "I" can now be written as:

$$I = \int_0^\infty \frac{e^{-k(h-z)} \sin(kx)}{k - k_0} dk = \frac{b \cdot c - a \cdot d}{c^2 + d^2} + C\pi e^{-k_0(h-z)} \cos(k_0 x) \quad (10)$$

Here, C is 2 for  $x \rightarrow +\infty$  and it is 0 for  $x \rightarrow -\infty$ , to satisfy the radiation condition given in Equation (4). The calculated a, b, c and d coefficients are given in the Appendix. They are taken from (Hess and Smith, 1966).

Now, if the kinematic boundary condition (zero normal velocity on flat-plate) is applied at three-quarter chord point of flat-plate, the following equation can be given as:

$$\frac{\partial \phi (x = \frac{c}{2} \cos \alpha, z = h - \frac{c}{2} \sin \alpha)}{\partial z} = -U(\sin \alpha)(\cos \alpha) \quad (11)$$

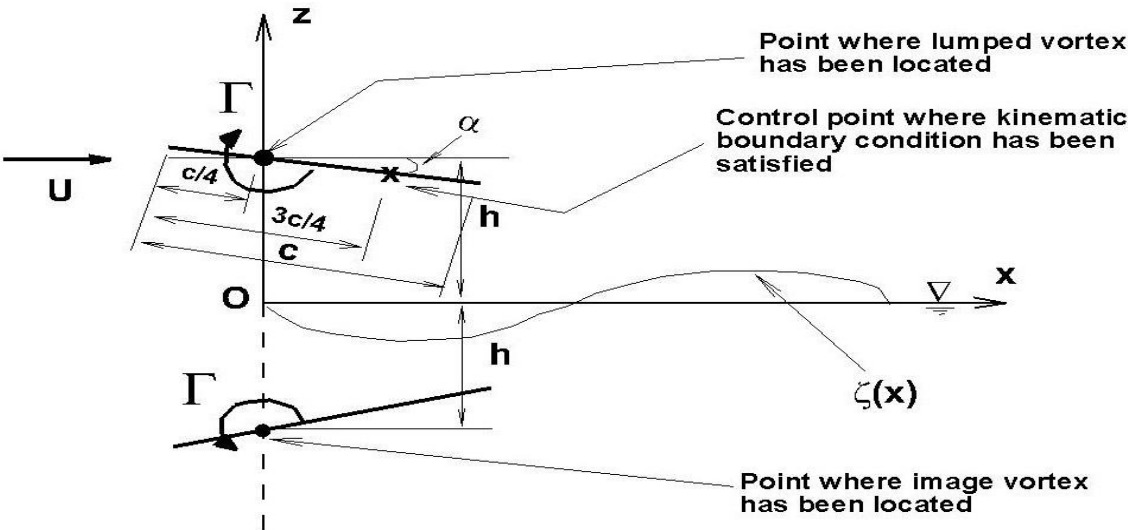


Figure 1. Definition of problem and coordinate system.

#### 4. Numerical Results and Discussion

First, the method has been validated with the results of NACA0004 foil section given in (Zong et al., 2012). Thickness ratio of foil is 0.04. The angle of attack is ( $\alpha=4^\circ$ ). Froude numbers ( $Fr_c = \frac{U}{\sqrt{gc}}$ ), are 15 and 18, and the corresponding ratios of clearance of flat-plate from free surface ( $h/c$ ) are 1.0 and 1.5, respectively. The lift coefficient  $C_L$  by present method is 0.53 at  $Fr_c=18$  and  $h/c=1.5$  while it is given as 0.53 in (Zong et al., 2012).

and if the circulation value for lumped vortex element in an unbounded flow domain (no free surface case)  $\Gamma_\infty$  is utilized:

$$\Gamma_\infty = \pi U c (\sin \alpha) \quad (12)$$

the following equation for circulation ratio can be obtained as:

$$\frac{\Gamma}{\Gamma_\infty} = \left( \frac{\cos \alpha}{c} \right) \left[ \frac{1}{2} \frac{x}{x^2 + (h-z)^2} + \frac{1}{2} \frac{x}{x^2 + (z+h)^2} + k_0 I \right]^{-1} \text{ at } \left( x = \frac{c}{2} \cos \alpha, z = h - \frac{c}{2} \sin \alpha \right) \quad (13)$$

Note that:

$$\frac{\Gamma}{\Gamma_\infty} = \frac{C_L}{C_{L\infty}} \quad (14)$$

Here,  $C_L$  is the lift coefficient of flat-plate with free surface effect and  $C_{L\infty}$ , the lift coefficient of flat-plate in unbounded flow domain (in case of no free surface effect), and  $C_{L\infty} = 2\pi(\sin \alpha)$ .

Furthermore, the wave elevation on the free surface can be calculated from Equation (3) as follows:

$$\frac{\zeta(x; z=0)}{c} = \frac{\Gamma}{\pi c} \left[ \frac{U}{g} \frac{h}{x^2 + (h)^2} + J/U \right] \text{ at } (x; z = 0) \quad (15)$$

where

$$J = \frac{a \cdot c + b \cdot d}{c^2 + d^2} - C\pi e^{-k_0(h)} \sin(k_0 x) \quad (16)$$

$\Gamma$  (circulation with free surface effect) is calculated by Equation (13).

The lift coefficient  $C_L$  by present method is 0.55 at  $Fr_c=15$  and  $h/c=1.0$  while it is 0.55 given in (Zong et al., 2012). This is a very strong validation of this analytical solution.

Later, the lift coefficient ratios versus Froude number at different clearance ratios by the present method have been shown in Figure 2. While the free surface causes an increase in lift coefficients of flat-plate for lower Froude numbers, it causes a decrease for higher Froude numbers (say  $Fr_c > 1$ ). Smaller clearance ratio makes this effect much clear. In Figure 3, the

variation of lift coefficient with Froude number as well as with the angle of attack of flat-plate is shown. Note that the differences due to angle of attack are indistinguishable.

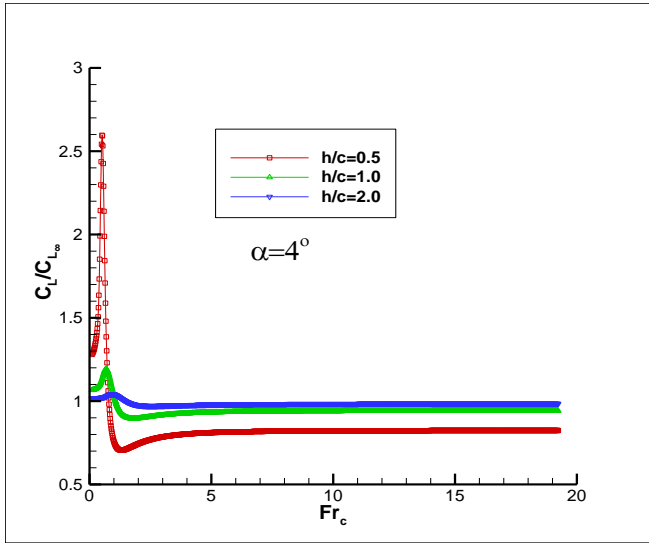


Figure 2. Lift coefficient ratio versus Froude number at different clearance ratios.

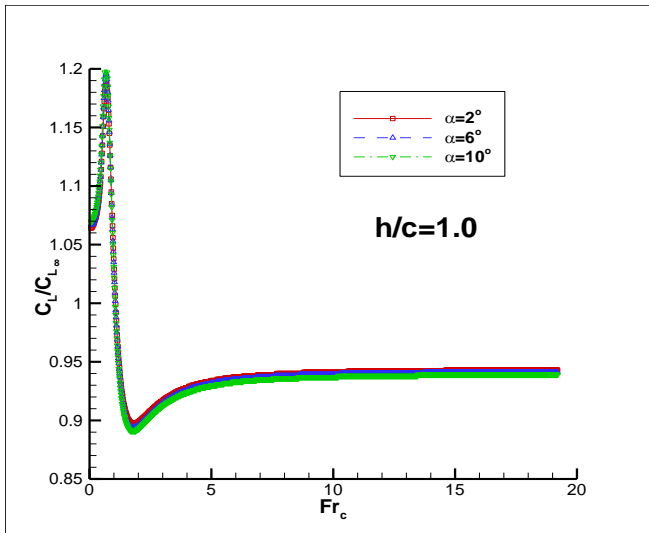


Figure 3. Lift coefficient ratio versus Froude number at different angles of attack.

In Figure 4, the change in wave elevation with Froude number has been demonstrated for a fixed clearance ratio at a fixed angle of attack. Note that as the Froude number increases, both the wave-height and wave-length become larger. This is consistent with those of given in (Larsson and Raven, 2010). In Figure 5, the change in wave elevation with clearance ratio has been demonstrated for a fixed Froude number and fixed angle of attack. As the clearance ratio decreases, the wave height increases but the wave-length becomes fixed. Finally, the effects of angle of attack on wave elevations have been shown in Figure 6. An increase in angle of attack for a fixed Froude number and fixed clearance ratio causes an increase in wave height but not in wave-length, which remains constant.

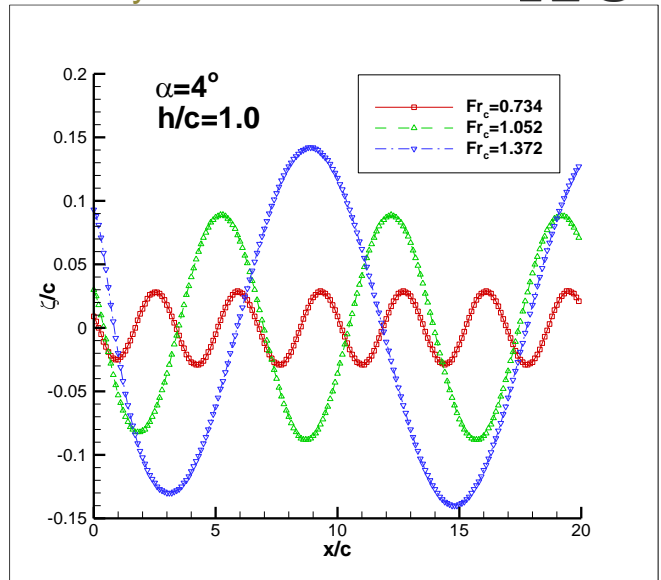


Figure 4. Variation of wave elevation with Froude number.

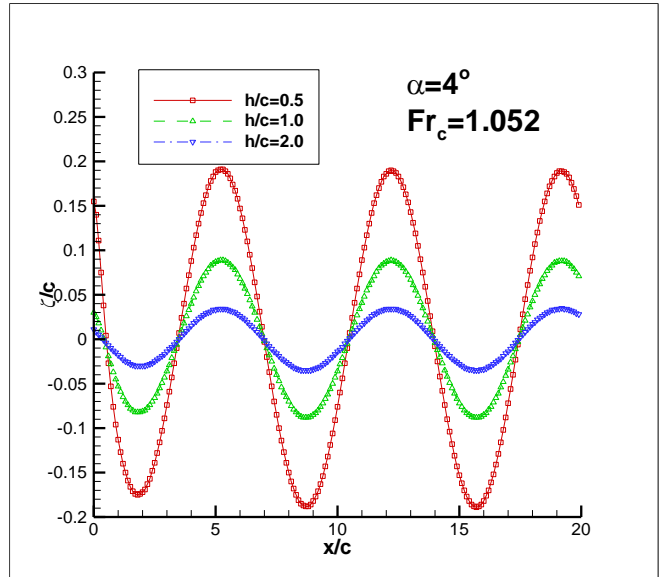


Figure 5. Variation of wave elevation with clearance ratios.

### 5. Conclusion

A closed-form solution has been developed for a flat-plate flying (moving) with a constant speed under a free surface. A hydrodynamic analysis has then been carried out for this problem. The flat-plate has been represented by a lumped vortex element. To the best of author's knowledge, there has been no such a study in literature before. An analytical solution has been obtained for lift coefficient and wave deformation on the free surface. The results by the present method were validated with those of another numerical method given in literature. The findings can be summarized as follows:

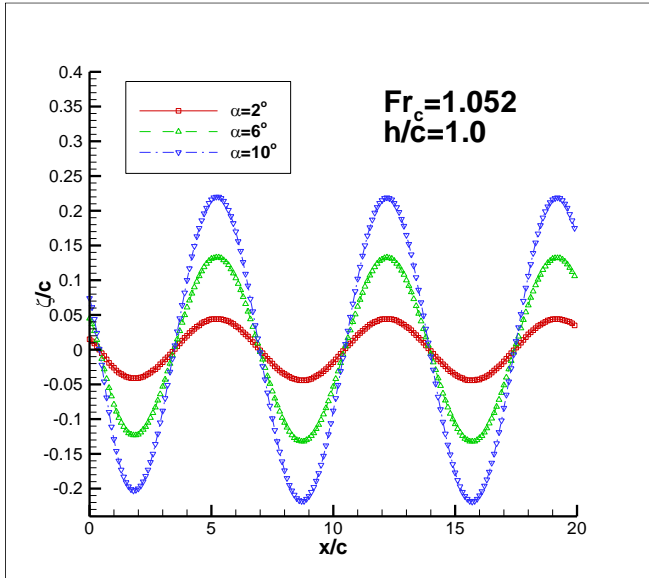


Figure 6. Variation of wave elevation with angle of attack.

- Free surface causes an increase in lift coefficient of flat-plate for lower Froude numbers. On the other hand, it causes a decrease for higher Froude numbers, (say greater than 1).
- An increase in Froude number causes an increase in wave height and wave-length.
- A decrease in clearance ratio from free surface causes an increase in wave height, but not in wave-length.
- An increase in angle of attack for a fixed Froude number and fixed clearance ratio from free surface causes an increase in wave height. But it causes no change in wave-length.

## 6. Nomenclature

c	chord
$C_L$	lift coefficient
$Fr_c$	Froude number
g	gravitational acceleration
h	clearance between flat-plate & free surface
$k_0$	wave number
p	ambient pressure
U	uniform incoming velocity
x	horizontal axis of coordinate system
z	vertical axis of coordinate system
$\alpha$	angle of attack
$\Gamma$	circulation
$\phi$	perturbation potential
$\Phi$	total potential
$\rho$	density of water
$\zeta$	wave elevation

## 7. Appendix

After the definitions of  $r = \sqrt{x^2 + (z-h)^2}$  and  $\beta = \tan^{-1}\left(\frac{x}{z-h}\right)$ , the following constants hold as given on pages 66-67 in the article by Hess and Smith (1966):

$$a = -[\ln(k_0 r) + 0.99999207\gamma + m_1 k_0 r (\ln(k_0 r) \cos\beta - \beta \sin\beta) + \gamma n_1 k_0 r \cos\beta + m_2 k_0^2 r^2 (\ln(k_0 r) \cos 2\beta - \beta \sin 2\beta) + \gamma n_2 k_0^2 r^2 \cos 2\beta + m_3 k_0^3 r^3 (\ln(k_0 r) \cos 3\beta - \beta \sin 3\beta) + \gamma n_3 k_0^3 r^3 \cos 3\beta + m_4 k_0^4 r^4 (\ln(k_0 r) \cos 4\beta - \beta \sin 4\beta) + \gamma n_4 k_0^4 r^4 \cos 4\beta + \gamma n_5 k_0^5 r^5 \cos 5\beta]$$

$$b = -[\beta + m_1 k_0 r (\ln(k_0 r) \sin\beta + \beta \cos\beta) + \gamma n_1 k_0 r \sin\beta + m_2 k_0^2 r^2 (\ln(k_0 r) \sin 2\beta + \beta \cos 2\beta) + \gamma n_2 k_0^2 r^2 \sin 2\beta + m_3 k_0^3 r^3 (\ln(k_0 r) \sin 3\beta + \beta \cos 3\beta) + \gamma n_3 k_0^3 r^3 \sin 3\beta + m_4 k_0^4 r^4 (\ln(k_0 r) \sin 4\beta + \beta \cos 4\beta) + \gamma n_4 k_0^4 r^4 \sin 4\beta + \gamma n_5 k_0^5 r^5 \sin 5\beta]$$

$$c = 1 + d_1 k_0 r \cos\beta + d_2 k_0^2 r^2 \cos 2\beta + d_3 k_0^3 r^3 \cos 3\beta + d_4 k_0^4 r^4 \cos 4\beta + d_5 k_0^5 r^5 \cos 5\beta + d_6 k_0^6 r^6 \cos 6\beta$$

$$d = d_1 k_0 r \sin\beta + d_2 k_0^2 r^2 \sin 2\beta + d_3 k_0^3 r^3 \sin 3\beta + d_4 k_0^4 r^4 \sin 4\beta + d_5 k_0^5 r^5 \sin 5\beta + d_6 k_0^6 r^6 \sin 6\beta$$

$$\gamma = 0.5772156649$$

$$m_1 = 0.23721365, m_2 = 0.0206543, m_3 = 0.000763297, m_4 = 0.0000097687$$

$$n_1 = -1.49545886, n_2 = 0.041806426, n_3 = -0.03000591, n_4 = 0.0019387339, n_5 = -0.00051801555$$

$$d_1 = -0.76273617, d_2 = 0.28388363, d_3 = -0.066786033, d_4 = 0.012982719, d_5 = -0.0008700861, d_6 = 0.0002989204$$

## 8. References

- Bal S. (2016). Free Surface Effects on 2-D Airfoils and 3-D Wings Moving Over Water. *Ocean Systems Engineering, An International Journal*, 6(3), 245-264.
- Bal S. (2018). Prediction of Hydrodynamic Performance of 3-D WIG by IBEM. *International Journal of Maritime Engineering (RINA Transactions Part A)*, 160, 249-256, 2018.
- Bal S, Kinnas SA. (2002). A Bem for the Prediction of Free Surface Effect on Cavitating Hydrofoils. *Computational Mechanics*, 28, 260-274.
- Bal S, Kinnas SA Lee H. (2001). Numerical Analysis of 2-D and 3-D Cavitating Hydrofoils under a Free Surface. *Journal of Ship Research*, 45(1), 34-49.
- Barber JT. (2007). A Study of Water Surface Deformation due to Tip Vortices of a Wing-in-Ground Effect. *Journal of Ship Research*, 51(2), 182-186.
- Dogru A, Bal S. (2016). Performance prediction of wings moving above free surface. *Advances in Boundary Element and Meshless Techniques XVII*, 85-92, Middle East Technical University, Ankara, Turkey, July 11-13.
- Gradshteyn IS, Ryzhik IM. (1965). Table of Integrals, Series and Products. NY, USA, Academic Press.
- Grundy I. (1986). Airfoils Moving in Air Close to a Dynamic Water Surface. *Journal of the Australian Mathematical Society Series B*, 27(3), 327-345.
- Hess JH, Smith AMO. (1966). Calculation of Potential Flow about Arbitrary Bodies. *Progress in Aeronautical Sciences*, 8, 1-138.

- Hu H, Ma D, Guo Y, Yang M. (2021). Airfoil Aerodynamics in Proximity to Wavy Water Surface. *Journal of Aerospace Engineering (ASCE)*, 34(2), 04020119.
- Katz J, Plotkin A. (2001). *Low Speed Aerodynamics: From Wing Theory to Panel Methods*. 2<sup>nd</sup> ed. New York, USA, McGraw-Hill International Book Company.
- Katz J. (2019). Convergence and Accuracy of Potential Flow Methods. *Journal of Aircraft*, 56, 2371-2375.
- Kinaci OK, Bal S. (2016). Performance prediction of 2D foils moving above and close to free surface. *Advances in Boundary Element and Meshless Techniques XVII*, 43-50, Middle East Technical University, Ankara, Turkey, July 11-13.
- Larsson L, Raven HC. (2010). *The Principles of Naval Architecture Series: Ship Resistance and Flow*. NY, USA, SNAME Publication.
- Liang H, Zhou L, Zong Z, Sun L. (2013). An Analytical Investigation of Two-Dimensional and Three-Dimensional Biplanes Operating in the Vicinity of a Free Surface. *Journal of Marine Science and Technology*, 18, 12-31.
- Liang H, Zong Z, Zou L. (2013). Nonlinear Lifting Theory for Unsteady
- WIG in Proximity to Incident Water Waves. Part 1: Two-Dimension. *Applied Ocean Research*, 43, 99–111.
- Matveev KI. (2013). Modeling of Finite-Span Ram Wings Moving Above Water of Finite Froude Numbers. *Journal of Ship Research*, 58(3), 146–156.
- Rozhdestvensky KV. (2006). Wing-in-Ground Effect Vehicles. *Progress in Aerospace Sciences*, 42, 211–283.
- Zhi H, Xiao T, Chen J, Wu B, Tong M, Zhu Z. (2019). Numerical analysis of aerodynamics of a NACA4412 airfoil above wavy water surface. *In AIAA aviation 2019 forum*, 3694. Reston, VA, American Institute of Aeronautics and Astronautics.
- Zong Z, Liang H, Zhou L. (2012). Lifting Line Theory for Wing-in Ground Effect in Proximity to a Free Surface. *Journal of Engineering Mathematics*, 74, 143-158.